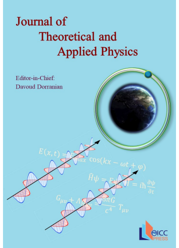

Volume 17, Issue 3, 172334 (1-6)

Journal of Theoretical and Applied Physics (JTAP)

https://dx.doi.org/10.57647/j.jtap.2023.1703.34

Theoretical modelling of terahertz acoustic wave generated by a femtosecond laser pulse in a dense plasma having density gradient

Sandeep[1,2]*, Hitendra K. Malik[1]*

[1]Plasma Science and Technology Laboratory, Department of Physics, Indian Institute of Technology Delhi, New Delhi, India.
[2]Department of Physics, Deen Dayal Upadhyaya College, University of Delhi, New Delhi, India.

***Corresponding author**: sandeep@ddu.du.ac.in; hkmalik@physics.iitd.ac.in

Received 07 November 2022; Accepted 16 January 2023; Published online 20 January 2023

Abstract:
Near the critical layer, a p-polarized laser that impinges on a dense plasma having density gradient at an angle to the density gradient transforms into a plasma wave. Even after the laser pulse has stopped, the plasma wave survives. The electrons close to the crucial layer are heated by the plasma wave. Increased plasma pressure and the production of ion-acoustic waves at frequencies lower than those of the ion plasma are the results of a sudden increase in plasma electron temperature. It appears to be a mechanism for ion-acoustic waves observed in an experiment (Adak et al. Phys. Rev. Lett. 114 (2015) 115001), where alternatively the plasma wave can excite ion acoustic waves in Terahertz frequency range via the decay instability. In the present work, we have theoretically demonstrated these observations.

Keywords: Ion acoustic wave; Plasma wave; Terahertz nature; Decay instability

1. Introduction

In physics and engineering, there is a long, rich, and fascinating history of the creation of acoustic waves in hydrodynamical systems. This varies from the comparatively banal issues related to jet engine acoustic wave generation and rocket propulsion [1–7]. Weak plasma that may spread shocks over vast stretches of space makes up interstellar space. Understanding shocks produced by supernova explosions and other astronomical events is crucial because they mix up the circumstellar matter, which has an impact on our understanding of the formation of stars and the evolution of galaxies. These phenomena are now possible in laboratories using powerful lasers; identical shocks can be produced and investigated experimentally. High power laser-solid interactions can be used to generate powerful shocks and blast waves at very high energy densities [8–11].
Numerous decades of research have revealed that electrostatic waves may be produced by parametric instabilities that can occur in a high-power laser. When a laser strikes an inhomogeneous plasma, the parametric decay, oscillating two-stream instabilities, and resonant absorption mechanism can increase absorption at the critical surface where the plasma frequency matches the laser frequency. The incident laser energy can decay into a light wave and either a low-frequency ion wave (stimulated Brillouin scattering) or an electron plasma wave (stimulated Raman scattering). The under-dense portions of the plasma will experience these instabilities, which will prevent laser energy from ever reaching the crucial surface where the improved absorption mechanisms may function [11–17].
Adak et al. [18] published their exciting experimental findings on the development of powerful terahertz acoustic waves by a femtosecond laser in a dense laser-produced plasma. In this experiment, a solid foil target was illuminated by a 20-terawatt laser (Ti: sapphire, 30 fs, 800 nm) with chirped pulse amplification, focused to a 15 μm spot size by an off-axis parabolic mirror at an angle of incidence of 45°. On a picosecond time scale, these phenomena were discovered in the interaction of a powerful ($\geq 10^{16}$ W/cm^2) femtosecond laser with dense plasma.
In this paper, we present our theoretical research into the hydrodynamic processes brought on by the plasma's rapid

heating by a fast electron beam. The pedestal was powerful enough to create plasma with small scale lengths despite the contrast ratio being $\sim 10^{-4}$. We present a different interpretation for these experiments in this work. The short pulse laser that is propagating in the p-polarization mode at an angle to the density gradient transforms into a Langmuir wave close to the critical layer (Schematic shown in Fig. 1. The Langmuir wave exhibits an Airy function field variation with scale length $\lambda_{es} = (L_n v_{th}^2/\omega_L^2)^{1/3}$ in a linear density profile with scale length L_n, where v_{th} is the electron thermal speed and ω_L is the laser frequency. By using Landau damping and inverse Bremsstrahlung on a short time scale with electron temperature scale length λ_{es}, the Langmuir wave heats the electrons. This sharp rise in local plasma pressure acts as a source for ion acoustic waves of frequency $\omega_{ac} \simeq (2\pi/\lambda_{es})c_s$, where c_s is the ion acoustic sound speed. In section 2, we estimate the amplitude of the Langmuir wave and the electron temperature rise. In section 3, we estimate the ion acoustic wave amplitude as it propagates down in the under-dense region.

2. Calculations for Langmuir wave and rise in electron temperature

Consider a plasma half space ($z > 0$) with equilibrium electron density n_0 a linear function of z; $z < 0$ is the free space. We assume the linear plasma density profile to satisfy the plasma frequency as $\omega_p^2 = \omega^2(z/L_n)$, At $z = L_n$ is the critical layer and ω_p^2 is the square of plasma frequency. A p-polarised laser pulse of energy E_L, pulse duration τ_L and frequency ω_L is obliquely incident on the plasma at an angle of incidence θ_i. In our treatment, we do not include the modification of electron density by nonlinear ponderomotive force. For mode conversion, one requires the component of wave field along the density gradient and the separation between the critical layer and turning point to be small.

Near to the critical layer, the short pulse laser that is moving in the p-polarization mode at an angle to the density gradient changes into a plasma wave of frequency ω. Let α be the fraction of laser energy converted into the plasma wave of associated electric field E_s and energy density W_{ES}. We also assume that after mode conversion the plasma wave has same cross section as that of laser pulse, πr_0^2; where r_0 is the pulse width parameter.

On conversion, a fraction α of laser pulse energy is transformed into plasma wave near the critical layer. Then from energy conservation the expression of energy density of both the waves is related as

$$\int W_{ES}\pi r_0^2 dz = E_L\alpha \tag{1}$$

The S.I. unit of α is Coulomb-metre. In the limit of weak fields, the current density $\mathbf{J}$ is a linear function of $\mathbf{E}$ .i.e.

$$\mathbf{J} = \sigma\mathbf{E}$$

where σ is the electrical conductivity.

For the amplitude ($\mathbf{E}_s$) of the electric field as a slowly varying function of time (as compared to the inverse of phase frequency) the current density reads

$$\mathbf{J}(t) = \sigma\mathbf{E} + i\frac{\partial\sigma}{\partial\omega}\frac{\partial\mathbf{E}_s}{\partial t}\ e^{-i\omega t}$$

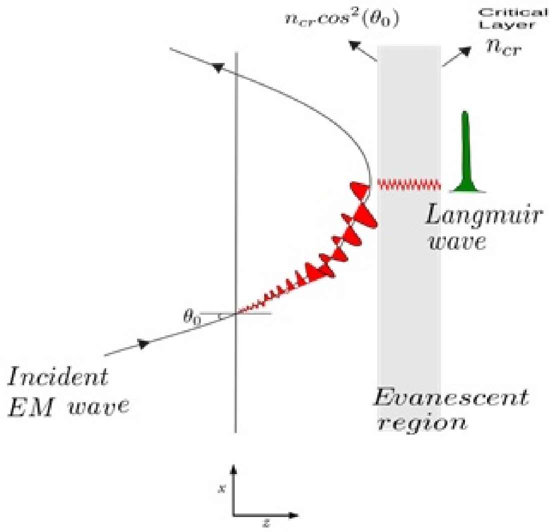

Figure 1. Schematic of the turning point and mode conversion layer.

In general, $\sigma = \sigma_r + i\sigma_i$, i.e. it has real and imaginary parts for higher frequency fields, and $\sigma_r \ll \sigma_i$. The term $\mathbf{J}\cdot\mathbf{E}$ is averaged over a time period $2\pi/\omega$

$$(\mathbf{J}\cdot\mathbf{E})_{av} = \frac{1}{2}\sigma_r|E_s|^2 - \frac{1}{4}\frac{\partial\sigma_i}{\partial\omega}\frac{\partial|\mathbf{E}_s|^2}{\partial t}$$

This is based on the comparison of the last two equations without magnetic field fluctuations. The expression of energy density of plasma wave is given by

$$W_{ES} = \omega\frac{\partial\varepsilon}{\partial\omega}\frac{\varepsilon_0|E_s|^2}{4} \tag{2}$$

where ε is the permittivity associated with the plasma wave and is given as

$$\varepsilon = 1 - \left(\frac{\omega_p^2 + 3k^2v_{th}^2}{\omega^2}\right)$$

The thermal velocity of the electrons in terms of electron temperature T_e is $v_{th} = \sqrt{T_e/m}$. From the above relation, we get

$$\frac{\partial\varepsilon}{\partial\omega} = \frac{2}{\omega}\frac{\omega_p^2 + 3k^2v_{th}^2}{\omega^2} \tag{3}$$

The Eq. (3) is reduced to $\partial\varepsilon/\partial\omega \simeq 2/\omega$ as $\omega^2 \simeq \omega_p^2 + 3k^2v_{th}^2$; Then Eq. (2) can be written as

$$W_{ES} \simeq \frac{\varepsilon_0|E_s|^2}{2} \tag{4}$$

For the electrostatic wave, the dispersive dielectric or permittivity, $\varepsilon_r(\omega,k) \cong 0$

$$\frac{\partial\varepsilon_r}{\partial k}\Delta k + \frac{\partial\varepsilon_r}{\partial\omega}\Delta\omega = 0$$

$$\frac{\partial\varepsilon_r}{\partial k} = \frac{\partial\varepsilon_r}{\partial\omega}\upsilon_g$$

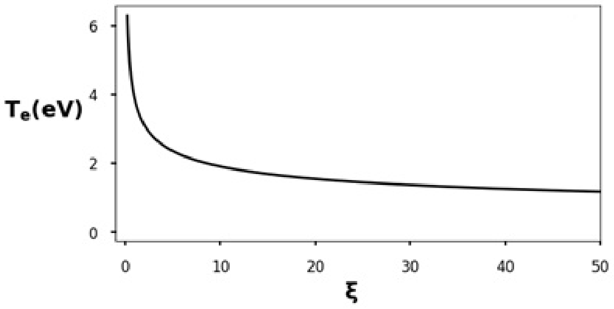

Figure 2. Thermal energy of electrons as function of parameter $\xi = z/\lambda_{es}$.

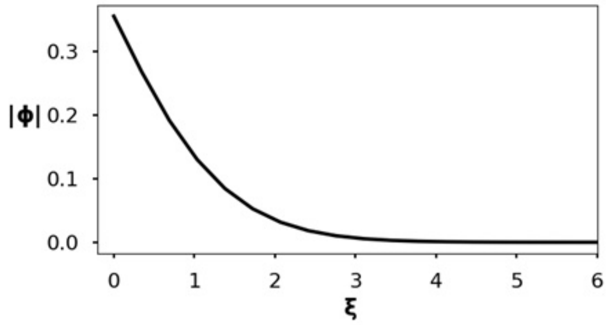

Figure 3. The amplitude of plasma potential φ as a function of normalized distance $\xi = z/\lambda_{es}$.

where $\upsilon_g = \Delta\omega/\Delta k$ is the group velocity of the wave and E_0 is the amplitude of the electric field of the plasma wave. Therefore, the net power flux entering the unit volume can be written as

$$P = \frac{1}{2}\omega\frac{\partial\varepsilon_r}{\partial\omega}\frac{E_0^2}{8\pi}\upsilon_g$$

This is the power flow density. One may recognize that P is the product of energy density (of the field and particle drift motion) and group velocity.

Through the conversion of laser energy into the plasma wave, the wave propagates down the density gradient. By using weak absorption approximation, the plasma wave power flow density can be assumed to be constant for a few scale lengths, then; $W_{ES}\upsilon_g = \text{constant} = c_1$. The υ_g group velocity is given by

$$\upsilon_g = \frac{\partial\omega}{\partial k} = \frac{3kv_{th}^2}{\omega}$$

then

$$W_{ES} = \frac{c_1}{\upsilon_g} = \frac{c_1\omega}{3kv_{th}^2} \tag{5}$$

From the dispersion relation of plasma wave: $\omega^2 \simeq \omega_p^2 + 3k^2v_{th}^2$

$$kv_{th} = \sqrt{\frac{\omega^2-\omega_p^2}{3}} \simeq \sqrt{\frac{2}{3}}\sqrt{\frac{\omega-\omega_p}{\omega}}\omega \quad \text{for} \quad \omega \simeq \omega_p$$

With the use of kv_{th} term, Eq. (5) becomes

$$W_{ES} = \frac{c_1}{\sqrt{6}v_{th}}\Big(\frac{\omega}{\omega-\omega_p}\Big)^{\frac{1}{2}} \tag{6}$$

Using Eq. (6) in Eq. (1), we get

$$\frac{c_1}{\sqrt{6}}\pi r_0^2\int\Big(\frac{\omega}{\omega-\omega_p}\Big)^{\frac{1}{2}}\frac{1}{v_{th}}dz = E_L\alpha \tag{7}$$

The energy of the electrostatic plasma wave is eventually absorbed by the electrons mainly by Landau damping and collisional damping. In our analysis, collisional damping is not considered here. In the analysis, the distribution function is modified by the plasma wave. This will happen when plasma particles which give rise to resonant wave particle interaction are responsible for damping of plasma waves. In this way, energy transfers from the plasma wave to electrons. If it is assumed that all the energy associated with the plasma wave is converted into electrons energy, then the thermal energy of electrons per unit volume $\simeq W_{ES}$. This will result into

$$\frac{3}{2}T_en_e \simeq W_{ES} = \frac{c_1}{\sqrt{6(\frac{T_e}{m})}}\Big(\frac{\omega}{\omega-\omega_p}\Big)^{\frac{1}{2}}$$

$$T_e = \Big(\frac{2}{27}\Big)^{\frac{1}{3}}m^{\frac{1}{3}}\Big(\frac{c_1}{n_e}\Big)^{\frac{2}{3}}\Big(\frac{\omega}{\omega-\omega_p}\Big)^{\frac{1}{3}} \tag{8}$$

Thus,

$$v_{th} = \sqrt{\frac{T_e}{m}} = \Big(\frac{2}{27}\Big)^{\frac{1}{6}}\Big(\frac{\omega}{\omega-\omega_p}\Big)^{\frac{1}{6}}m^{-\frac{1}{3}}\Big(\frac{c_1}{n_e}\Big)^{\frac{1}{3}} \tag{9}$$

Using this in Eq. (7)

$$\frac{c_1}{\sqrt{6}}\pi r_0^2\int\Big(\frac{\omega}{\omega-\omega_p}\Big)^{\frac{1}{3}}\Big(\frac{c_1}{n_e}\Big)^{\frac{1}{3}}\Big(\frac{27}{2}\Big)^{\frac{1}{6}}m^{\frac{1}{3}}dz = E_L\alpha$$

$$c_1^{\frac{2}{3}} = \frac{E_L\alpha}{\pi r_0^2 m^{\frac{1}{3}}2^{\frac{2}{3}}}\;\frac{1}{\int\big(\frac{\omega}{\omega-\omega_p}\big)^{\frac{1}{3}}n_e^{\frac{1}{3}}dz} \tag{10}$$

In terms of laser intensity, $I_L = E_L/(\tau_L\pi r_0^2)$, the expression of c_1 is reduced to

$$c_1 = \Big(\frac{I_L\tau_L\alpha}{m^{\frac{1}{3}}2^{\frac{2}{3}}}\Big)\frac{1}{\Big(\int\big(\frac{\omega}{\omega-\omega_p}\big)^{\frac{1}{3}}n_e^{\frac{1}{3}}dz\Big)^{\frac{3}{2}}} \tag{11}$$

Using c_1 from Eq. (11) in Eq. (8), we get

$$T_e = \Big(\frac{\omega}{\omega-\omega_p}\Big)^{\frac{1}{3}}\Big(\frac{2^{-\frac{1}{3}}I_L\tau_L\alpha}{3n_e^{\frac{2}{3}}}\Big)\Big(\frac{1}{\int\big(\frac{\omega}{\omega-\omega_p}\big)^{\frac{1}{3}}n_e^{\frac{1}{3}}dz}\Big) \tag{12}$$

For linear density profile $\omega_p^2 = \omega^2(z/L_n)$, $z = L_n$ is the critical layer, as mentioned earlier. The integral in the denominator of Eq. (12) can be written as

$$\int_0^{L_n}\Big(\frac{\omega}{\omega-\omega_p}\Big)^{\frac{1}{3}}n_e^{\frac{1}{3}}dz = 3L_n\,n_{cr}^{\frac{1}{3}} \tag{13}$$

Substituting Eq. (13) in Eq. (12), we get

$$T_e = \frac{I_L\tau_L\alpha}{9n_{cr}L_n}\Big(1-\frac{z}{L_n}\Big)^{-\frac{1}{3}} \tag{14}$$

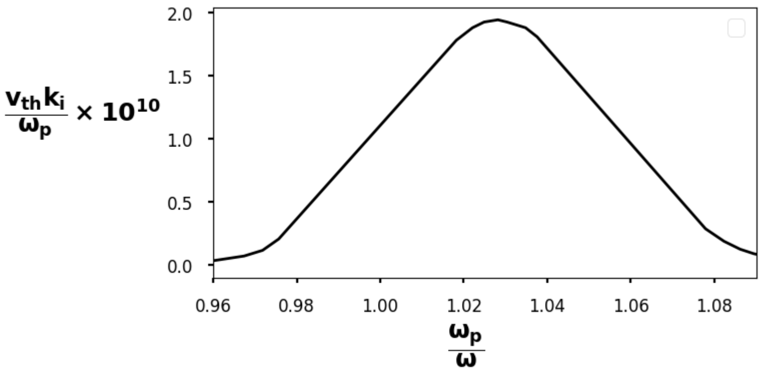

Figure 4. Dimensionless propagation vector ($v_{th}k_i/\omega_p$ versus dimensionless frequency ω_p/ω

By substituting z in terms of dimensionless parameter ξ, Eq. (14) reduces to

$$T_e = \frac{I_L \tau_L \alpha}{9 n_{cr} L_n}\left(1 - \frac{\xi}{L_n}\left(\frac{L_n T_e}{\omega_L^2 m}\right)^{\frac{1}{3}}\right)^{-\frac{1}{3}} \tag{15}$$

The parameters used in the analysis are as $I_L = 10^{18}$ W/cm^2, $\tau_L = 30\times 10^{-15}$ sec, $\alpha = 0.1$, $n_{cr} = 2\times 10^{21}$ cm^{-3} and $L_n = 30$ μm.
The electron temperature T_e to its Fourier transform temperature T_{ek} is related as per following equation

$$T_e = \frac{1}{\sqrt{\pi}}\int_{-\infty}^{\infty} T_{ek}\ e^{ikz} dz$$

and

$$T_{ek} = \frac{1}{\sqrt{2\pi}}\int_{-\infty}^{\infty} T_e\ e^{-ikz} dz$$

As T_e to be localized between $z = 0$ to L_n, then its spatial width can be obtained as

$$T_e \sim E_s^2$$

The electron temperature varies in the scale length of $\lambda_{es} = (L_n v_{th} r/\omega_p^2)^{1/3}$, where the initial temperature is used in the normalization through the thermal velocity. The plot of variation of thermal energy of electrons with respect to normalized distance z is shown in Fig. 2. Here it is evident that the plasma wave loose its energy to electrons at a small length scale near the critical layer (means the rate is faster) and the electron temperature is high near the critical layer. So, it implied that sudden change in temperature leads to large gradient in the electron density. This change in density is responsible for the acoustic wave generation in plasma.

3. Ion acoustic wave evolution in THz frequency range

Now the analysis can be done by taking into consideration of the plasma wave potential, φ.
Again, considering the plasma wave in a density gradient of the form,

$$\omega_p^2 = \omega^2\left(1 + \frac{z}{L_n}\right)$$

The Langmuir wave dispersion relation is $\omega^2 = \omega_p^2 + 3k^2 v_{th}^2$. Based on this, we can also write

$$k^2\varphi = \frac{\omega^2 - \omega_p^2}{3v_{th}^2}\varphi$$

or

$$\frac{d^2\varphi}{dz^2} + \frac{\omega^2 - \omega_p^2}{3v_{th}^2}\varphi = 0$$

This can be further modified as

$$\frac{d^2\varphi}{dz^2} - \frac{\omega^2}{3v_{th}^2 L_n} z\varphi = 0 \tag{16}$$

In terms of dimensionless quantities $(3v_{th}^2 L_n/\omega^2)^{1/3} = \lambda_{es}$, $z/\lambda_{es} = \xi$; Eq. (16) takes the form

$$\frac{d^2\varphi}{d\xi^2} - \xi\varphi = 0 \tag{17}$$

The solution of Eq. (17) can be written in terms of Airy function

$$\varphi = A_s A_i(-\xi) e^{-i\omega t} \tag{18}$$

The variation of this potential is shown in Fig. 3, where it is evident that the fall in the plasma potential is similar to the Airy function, and it is showing the large potential in small region of normalized distance. The particles lying in this potential region will gain energy in a large extent, resulting in a large pressure gradient. As the plasma wave propagates into plasma, due to resonant interaction with the plasma species via Landau damping, it results into gain of energy to electrons.
From Eq. (18), the temporal damping rate Γ and spatial damping rate k_i are related by the following equation

$$2\Gamma\omega = 6kk_i v_{th}^2$$
$$k_i = \frac{\Gamma}{3kv_{th}^2}\omega \simeq \frac{\Gamma}{\sqrt{3}}\left(\frac{\omega}{v_{th}\sqrt{\omega^2 - \omega_p^2}}\right)$$

This can be seen that k_i reduces to the following simple form

$$k_i = \frac{\omega_p}{v_{th}\sqrt{3}}\left(\frac{\omega_p^4}{(\omega^2 - \omega_p^2)^2}\right)\ e^{-\frac{\omega_p^2}{\omega^2 - \omega_p^2}}$$

Fig. 4 shows that the absorption of energy by the electrons from the plasma wave is high just near the critical layer. As electron and ion motions are not independently controlled, the change in electron density is expected to cause a variation in the ion density. But the electrons are the species which show the fast response compared to the ions. The rise in plasma temperature in the small and localized region near the critical layer due to sudden rise in the electron temperature gives rise to large oscillations in the ion density. The ion density oscillations give rise to the excitation of ion acoustic wave, corresponding to which the wave number in localized region is written as

$$k_{ac} \sim \frac{2\pi}{\lambda_{es}} = \Big(\frac{\omega_p^2}{L_n v_{th}^2}\Big)^{\frac{1}{3}} \simeq \frac{\omega_L}{c}\Big(\frac{c^3}{L_n v_{th}^2 \omega_L}\Big)^{\frac{1}{3}}$$

We calculate the sound frequency using the parameters: $L_n\omega_L/c = 2\pi L_n/\lambda_0 = 60$ and $k_{ac} \sim \omega_L/c(100/60)^{1/3} \sim \omega_L/c$ in the dispersion relation as

$$\omega_{ac} = k_{ac}c_s = \omega\frac{c_s}{c} = 2\times 10^{15}\times\frac{1}{650} = 3\times 10^{12}\text{rad/sec}$$

Clearly the value 3×10^{12} rad/sec of the frequency of ion acoustic wave is in Terahertz range. This explains the possible phenomenon of Terahertz acoustic wave generation by a femtosecond laser pulse in a dense plasma having density gradient.

4. Conclusion

In the present scheme, a short pulse laser moving in the p-polarization mode at an angle to the density gradient is found to convert into a Langmuir wave or plasma wave. In a linear density profile with scale length L_n, this wave displays an Airy function field variation with a scale length of $\lambda_{es} \sim 20\ \mu$m. The Langmuir wave heats the electrons utilising Landau damping and inverse Bremsstrahlung on a short time scale with electron temperature scale length λ_{es}. Ion acoustic wave with the frequency $\omega_{ac} \simeq 3\times 10^{12}$ rad/sec is generated as a result of this abrupt increase in local plasma pressure when the laser with frequency 2×10^{15} rad/sec is launched in a plasma having strong density gradient with density scale length of 9 μm.

Acknowledgements:
The author Yetendra Prasad Jha thanks the UGC-CSIR (Government of India) for supporting this work financially.

Conflict of interest statement:
The authors declare that they have no conflict of interest.

References

[1] L. Malik, S. Rawat, M. Kumar, and A. Tevatia. "Simulation studies on aerodynamic features of Eurofighter Typhoon and Dassault Rafale combat aircraft". *Materials Today: Proceedings*, **38**:191, 2021.

[2] L. Malik and A Tevatia. "Comparative Analysis of Aerodynamic Characteristics of F16 and F22 Combat Aircraft using Computational Fluid Dynamics". *Defence Science Journal*, **71**:137, 2021.

[3] H. K. Malik. "Terahertz radiation generation by lasers with remarkable efficiency in electron–positron plasma". *Physics Letters A*, **379**:2826, 2015.

[4] H. K. Malik. "Generalized treatment of skew-cosh-Gaussian lasers for bifocal terahertz radiation". *Physics Letters A*, **384**:126304, 2020.

[5] A. K. Malik and H. K. Malik. "Tuning and focusing of terahertz radiation by DC magnetic field in a laser beating process". *IEEE Journal of Quantum Electronics*, **49**:232, 2013.

[6] H. K. Malik and A. K. Malik. "Tunable and collimated terahertz radiation generation by femtosecond laser pulses". *Applied Physics Letters*, **99**:251101, 2011.

[7] A. K. Malik, H. K. Malik, and U. Stroth. "Terahertz radiation generation by beating of two spatial-Gaussian lasers in the presence of a static magnetic field". *Physical Review E*, **85**:016401, 2012.

[8] D. Singh and H. K. Malik. "Terahertz generation by mixing of two super-Gaussian laser beams in collisional plasma". *Physics of Plasmas*, **21**:083105, 2014.

[9] H. K. Malik and S. Punia. "Dark hollow beams originating terahertz radiation in corrugated plasma under magnetic field". *Physics of Plasmas*, **26**:063102, 2019.

[10] H. K. Malik and R. Gill. "Control of peaks of terahertz radiation and tuning of its frequency and intensity". *Physics Letters A*, **382**:2715, 2018.

[11] H. K. Malik. *Laser-Matter Interaction for Radiation and Energy*. CRC Press, 1th edition, 2021.

[12] R. Gill, D. Singh, and H. K. Malik. "Multifocal terahertz radiation by intense lasers in rippled plasma". *Journal of Theoretical and Applied Physics*, **11**:103, 2017.

[13] H. K. Malik, T. Punia, and D. Sharma. "Hat-Top Beams for Generating Tunable THz Radiations Using a Medium of Conducting Nanocylinders". *Electronics*, **10**:3134, 2021.

[14] L. Malik. "Dark hollow lasers may be better candidates for holography". *Optics and Laser Technology*, **132**:106485, 2020.

[15] L. Malik and A. Escarguel. "Role of the temporal profile of femtosecond lasers of two different colours in holography". *EPL (Europhysics Letters)*, **124**:64002, 2019.

[16] L. Malik, A. Escarguel, M. Kumar, A. Tevatia, and R. S. Sirohi. "Uncovering the remarkable contribution of lasers peak intensity region in holography". *Laser Physics Letters*, **18**:086003, 2021.

[17] A. Adak, D. R. Blackman, G. Chatterjee, P. K. Singh, A. D. Lad, P. Brijesh, A. P. L. Robinson, J. Pasley, and G. R. Kumar. "Ultrafast dynamics of a near-solid-density layer in an intense femtosecond laser-excited plasma". *Physics of Plasmas*, **21**:062704, 2014.

[18] A. Adak, A. P. L. Robinson, P. K. Singh, G. Chatterjee, A. D. Lad, J. Pasley, and G. R. Kumar. "Terahertz Acoustics in Hot Dense Laser Plasmas". *Phys. Rev. Lett.*, **114**:115001, 2015.